Eur. Phys. J. Spec. Top.
https://doi.org/10.1140/epjs/s11734-024-01087-5

THE EUROPEAN PHYSICAL JOURNAL SPECIAL TOPICS

Regular Article

Dark photons from displaced vertices

Triparno Bandyopadhyay[a]

Department of Physics and Nanotechnology, College of Engineering and Technology, SRM Institute of Science and Technology, SRM Nagar, Kattankulathur 603203, Tamil Nadu, India

Received 17 September 2023 / Accepted 3 January 2024

Abstract We investigate the unexplored regions of the dark photon parameter space to find a search strategy suitable to probe these. We show how displaced track searches at colliders with large 4pi trackers around the interaction point are excellent choices for exploring these uncharted regions. As an example, we study in detail the sensitivity of the Belle II trackers to dark photons which mediate interactions between the visible and dark sectors. We also show that the same strategy can be employed by other experiments to achieve the same goal.

1 Introduction

With supersymmetry and exotica searches at the Large Hadron Collider (LHC) experiments returning nothing but exclusion plots for the last decade [1–5], the interest of the particle physics community has shifted substantially towards light, $\ll 1$ GeV particles. It is here that physics related to axion-like particles [6–11], dark photons (DP) [12–14], $L_i - L_j$ / $B - L$ bosons [15–18], the dark QCD spectrum [19], protophobic bosons [20, 21], etc. have captured the imagination of the community. Needless to say, this interest is not spurious as these hypothetical particles are invoked as solutions to many open questions in physics. These include, but are not limited to, the mediation between the visible and the dark sector [22–26], the muon $g-2$ puzzle [27], the ATOMKI 17 MeV anomaly [28, 29], the W-mass tension [30, 31], and the presently subdued—but never disappearing—flavor anomalies [32].

In this note, we will be concentrating on light ($\sim$ MeV) vector bosons with vectorial couplings to the standard model (SM) fermions. Models that belong to this category are varied and multifaceted; however, owing to the vectorial nature of their couplings, these can be parametrised in somewhat generalised fashion. The prototypical model that represents this vast array of models is the dark photon which interacts with the SM fermions through gauge kinetic mixing with the photon [12–14]. The dark photon (DP), starting out as a theoretical curiosity, has gained a central role in modern particle physics research due to its potential to be a simple (and predictive) portal to the dark sector of the Universe. In this paper, we vary the relative coupling strength of the DP between the visible and the dark sector NEW Z-prime Phenomenology. to define different model benchmarks.

Our aim in this paper is to discuss the sensitivity of the Belle II [33] experiment to the DP parameter space. To be specific, we are interested in displaced vertex searches that looks for long-lived dark DPs. This choice is informed by the observation that the region of parameter space that is as of now unexplored lies between those from recent prompt searches at different colliders [34–42] sensitive to strong (relatively) couplings, and searches at different beam dump experiments [43–52], sensitive to very weak couplings. The region of intermediate coupling strengths lends itself readily to displaced vertex searches at modern $\sqrt{s} \sim 10$ GeV colliders, constructed primarily to test flavor observables [33, 53, 54].

The results in this paper, in principle new, should be considered as an addendum to Ref. [55]. We employ the same analysis techniques developed in that paper. In this work, we extend the results Ref. [55] by looking at a different kind of model that does have couplings, varying from weak to strong, to the dark sector. As a result of this, not only do our exclusions change, but the existing constraints also change in nature.

The paper is organised as follows: in Sect. 2, we lay down our parametrization and compute the relevant decay widths and branching ratios. In Sect. 3, we discuss the analysis techniques employed to compute the sensitivity of the detector to the displaced vertices, leading to the 90% CL exclusions. Then, in Sect. 4, we show the exclusions

[a] e-mail: triparnb@srmist.edu.in (corresponding author)

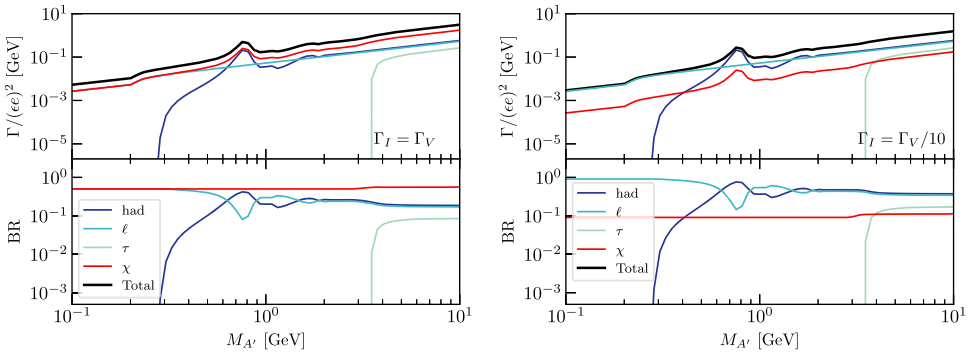

Fig. 1 For two different benchmarks, $\Gamma_I = \Gamma_V$ (left) and ii) $\Gamma_I = \Gamma_V/10$ (right), we plot the decay widths and branching rations of the dark photon to leptons, hadrons, the tau, and the dark sector

obtained for the different model benchmarks and discuss the qualitative nature of the contours. Then, in Sect. 5, we discuss the existing exclusions, from prompt and displaced searches. In this section, for completeness, we also discuss some prospects of displaced vertex searches at upcoming or existing experiments. Finally, we conclude.

2 The Model

Given we are working with a DP (A'), the couplings to the visible sector are unambiguously determined by those of the photon [12–14]. The DP couples to the SM particles with a strength that is scaled down—by a factor ϵ—from that of the photon and the scaling is the same for all the SM particles. However, neither the strength of the DP coupling to the dark sector, nor the structure of the dark sector are known. To take this into account, we write a general Lagrangian

$$\mathcal{L} \supset \epsilon e \left(\sum_f q_f \bar{f} \gamma^\mu f + \sum_\chi C_\chi \mathcal{O}^\mu_\chi \right) A'_\mu \,. \tag{1}$$

Here, C_χ are the couplings of the DP to dark sector operators O_χ. We parametrise the dark sector by ratios of decay width between the visible and the dark sector. The decay width of the DP to the visible sector is

$$\Gamma_V = \sum_f \Gamma_f = \sum_f n_f^c \frac{\epsilon^2 e^2 q_f^2}{12\pi} M_{A'} \sqrt{1 - 4\frac{m_f^2}{{M'_A}^2}} \left(1 + 2\frac{m_f^2}{{M'_A}^2}\right). \tag{2}$$

Here, n_f^c is the color factor of the fermion f. We then take three model benchmarks, defined in terms of the decay width to the visible sector, Γ_V and that to the invisible sector, Γ_I: (i) $\Gamma_I = \Gamma_V$, (ii) $\Gamma_I = 10\,\Gamma_V$, and (iii) $\Gamma_I = \Gamma_V/10$. Note, in this way, we can effectively parametrise the dark sector without requiring any specific information about it. Not, as for this displaced vertex search, we only need the cross-section of production of the DP and its branching ratios to leptons, the analysis is blind to details of the dark sector except the width.

In Fig. 1, we plot the partial widths and branching ratios of the dark photon to different final states. As we will see later, the kinematics of the process allow neither the τ leptons nor the hadrons to play any part. Note that the widths as depicted in Fig. 1 are quite large.[1] However, the decay widths, as plotted, are for the effective coupling, ϵe, taken to be one. For the region that we are interested in, $\epsilon e \ll 1$, the decay widths are scaled down well below the mass of the DP. For the decay width of the DP below $\Lambda_{\rm QCD}$, we use the package `DarkCast` [56] which uses the framework of Vector Meson Dominance [57] to take care of the hadronic thresholds.

With the details of our model laid out, we discuss the analysis strategy to look for the DPs in the next section.

[1] Even more so for the $\Gamma_I = 10\Gamma_V$ case which has not been shown in the figure.

3 The analysis

Our strategy to probe the parameter space of the DP is to look for displaced vertex signatures once (if) it is produced. We get a displaced vertex is when a particle produced at the interaction point (IP) travels a distance away from it before decaying, to charged decay products for our case. Tracing the tracks of the decay products, the vertex is reconstructed. Following the techniques employed in Ref. [55], we construct the vertex reconstruction efficiency (VRE) distribution as a function of the detector parameters and the kinematics of the process.

Let us assume that a particle is coming out at an azimuthal angle θ, measured from the z-axis (along the electron beam). If it decays at a distance l from the IP, then the distances along the z axis and the x-axis are $z = l\cos\theta$ and $r = l\sin\theta$, respectively. If this decay event is within the fiducial volume of the tracker, then it is accepted with some efficiency. For our purpose, the fiducial volume is defined not by the extent of the detector but also by that of efficient track reconstruction and background control.

In the left panel of Fig. 2, we show a cartoon that shows the relevant parameters involved. We show a section of the upper half of the tracking detector. A certain length in the x direction falls inside the beam pipe and hence is not accessible. Typically, immediately after the beam line are the silicon vertex trackers (pixel and strip) with the highest tracking resolution [33]. However, this region is dominated by vertices from long-lived SM decays like those of the Λ and the K_L. There are also tracks from the secondary interactions of particles with the detector material. Hence, we look for NP signals farther away from the IP, in the central drift chamber (CDC). This results in the lower cut on the radial distance, $r_{\rm min}$. The upper limit exists to ensure that the DP decays deep enough inside the tracker for the daughter particles to be reconstructed. The cuts in the axial length and in the azimuthal angle come from the consideration of the detector and beam pipe dimensions. The (r, z, θ) triad forms the set of relevant of geometric cuts.

For an event that passes the geometric cuts, we look at the efficiency of reconstruction of the vertex. From the detector side, there is a linearly falling efficiency (obtained from Monte Carlo simulations) with increasing radial distance [58]

$$\mathcal{E}(r) = \frac{r_{\rm max} - r}{r_{\rm max} - r_{\rm min}}\,. \tag{3}$$

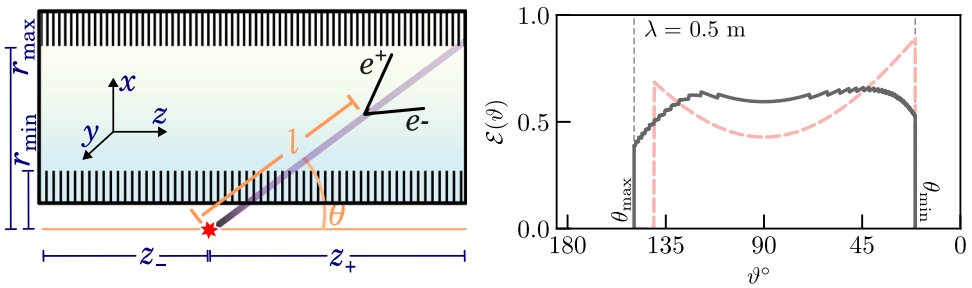

Fig. 2 *Left:* We plot a schematic of the Belle II tracker. We do not distinguish between the silicon inner detectors (VXD) and the drift chamber (CDC). We show the radial and axial limits within which a decay has to take place for which to accept an event. The gradient in the body of the detector represents the falling efficiency of detection away from the IP and the gradient in the outgoing particle represents the exponentially falling decay probability distribution. The coordinate system has also been shown. Details can be found in the text. *Right:* We show [55] the Vertex Reconstruction Efficiency distribution as a function of the scattering angle. In black, we show the true distribution, and in orange, we show the distribution we would have obtained if instead of convolution with the exponential decay distribution we assumed the particle to decay at its characteristic decay length ($\lambda = 0.5$ cm for this plot.). We also show the cuts imposed on the scattering angle. The vertical dashed lines (gray) show the cuts imposed on the scattering angle

Table 1 Relevant cuts for our analysis and other relevant details of the Belle II experiment (for justifications for the cuts, see Ref. [55])

$\sqrt{s}$	Integrated luminosity	Cuts			
		Radial (cm)	Axial (cm)	Angular	p_T
10.6 GeV	50 ab^{-1}	$10 < r < 80$	$-40 < z < 120$	$17^\circ < \theta < 130^\circ$	> 0.98 GeV

In addition, we impose a lower cut on p_T, $p_T^{\min}$, as the vertex reconstruction efficiency drastically falls with very low momentum. These cuts, along with other details of the Belle II detector, are tabulated in Fig. 1.

Given the relevant cuts, we construct the VRE distribution as follows. After being produced, the dark photon decays at a distance l from the IP with a probability of

$$\mathcal{P}(l) \;=\; \exp[-l/\lambda]/\lambda\,, \tag{4}$$

where λ is the characteristic decay length of the dark photon, given by

$$\lambda = \;\beta\gamma c\tau \;=\; \frac{|\vec{p}(M_{A'})|}{M_{A'}} c\tau(M_{A'},\,\epsilon e)\,, \tag{5}$$

where c is the velocity of light in vacuum and $\tau(M_{A'},\,\epsilon e)$ is the lifetime of the DP as a function of its mass and coupling strength. Therefore, the efficiency that a DP emitted in the direction θ will be detected at a length l from the IP is given by

$$\begin{aligned}
&\mathcal{E}_f(\theta) = \frac{\varepsilon_f}{\mathcal{N}} \int_{l_{\min}}^{l_{\max}} \frac{r_{\max} - l\,s\theta}{r_{\max} - r_{\min}} e^{-l/\lambda}\, \overline{\Theta}(l)\; dl\,,\\
&\text{where}\quad \overline{\Theta}(l) = \Theta(l\,s\theta - r_{\min})\,\Theta(r_{\max} - l\,s\theta)\,\Theta(l\,c\theta - z_{\min})\,\Theta(z_{\max} - l\,c\theta)\;,\\
&\text{and}\quad l_{\min} = r_{\min};\; l_{\max} = \sqrt{r_{\max}^2 + z_{\max}^2},\quad \mathcal{N} = \int_{l_{\min}}^{l_{\max}} e^{-l/\lambda}\,\overline{\Theta}(l)\; dl.
\end{aligned} \tag{6}$$

Note, with $s\theta \equiv \sin\theta$, $c\theta = \cos\theta$, $ls\theta$ and $lc\theta$ give the displacement of the DP in the radial and the axial direction, respectively. The ε_f factor is an overall detection efficiency of the lepton f (electron or muon for us), given by [33, 55]

$$\varepsilon_e \;=\; 0.93\,; \quad \text{and} \quad \varepsilon_\mu \;=\; 0.86\,. \tag{7}$$

Then, the total number of accepted displaced events over the full run of Belle II is given by

$$N_{\rm Tot} = L_{\rm I} \times \sum_f \int_{c\theta\min}^{c\theta_{\max}} dc\theta\; \frac{d\sigma}{dc\theta} \times {\rm BR}_f \times \mathcal{E}_f(\eta) \times \Theta\big(p_T^{\min} - \sin\vartheta(\eta)\,|\vec{p}|\big), \tag{8}$$

where L_I is the integrated luminosity, ${\rm BR}_f$ is the branching ratio in the f channel, $\mathcal{E}_f(\eta)$ is the VRE distribution for the f channel. The Heaviside function ensures that the p_T of the DP is greater than $p_T^{\min}$. We are not including the details of the differential cross-section, $\frac{d\sigma}{dc\theta}$, here as the details can be found in Ref. [55]. In the next section, we use the expression in Eq. (8) to estimate the reach of the Belle II detector towards the model benchmarks in question.

4 Results

For a particular point in the $(M_{A'},\,\epsilon e)$ plane, we require the total number of events [Eq. (8)] to be greater than three for that point to be accepted. This is because in a virtually background-free environment, Poisson statistics requires 2.3 events for exclusion at 90% CL.[2]

In Fig. 3, we plot the contours for the three cases discussed in Sect. 2, viz., $\Gamma_I = \Gamma_V/10$, $\Gamma_I = \Gamma_V$, and $\Gamma_I = 10\Gamma_V$. We also show a comparison between the exclusions at different integrated luminosities, the projected 50 ab^{-1} and the current ($\sim$) 200 fb^{-1}. From the figures, it is clear that when the branching to the visible sector is substantial, Belle II is sensitive to a large part of the $(M_{A'},\,\epsilon e)$ parameter space below 500 MeV, with effective couplings as small as 10^{-6} being probed. Note that the upper bound on the sensitivity is somewhat robust against change of branching ratios. However, the lower limit changes drastically with varying branching ratios.

The hatched region to the far left of all the plots marks the bound for electrophilic light particles from BBN and CMB observables [59]. The other shaded regions in the plots are existing exclusions on the parameter space

[2] The conservative lower limit on the radial distance, $r > 10$ cm, that we allow ourselves effectively vetoes SM backgrounds from K_L and Λ decays and those from secondary interactions.

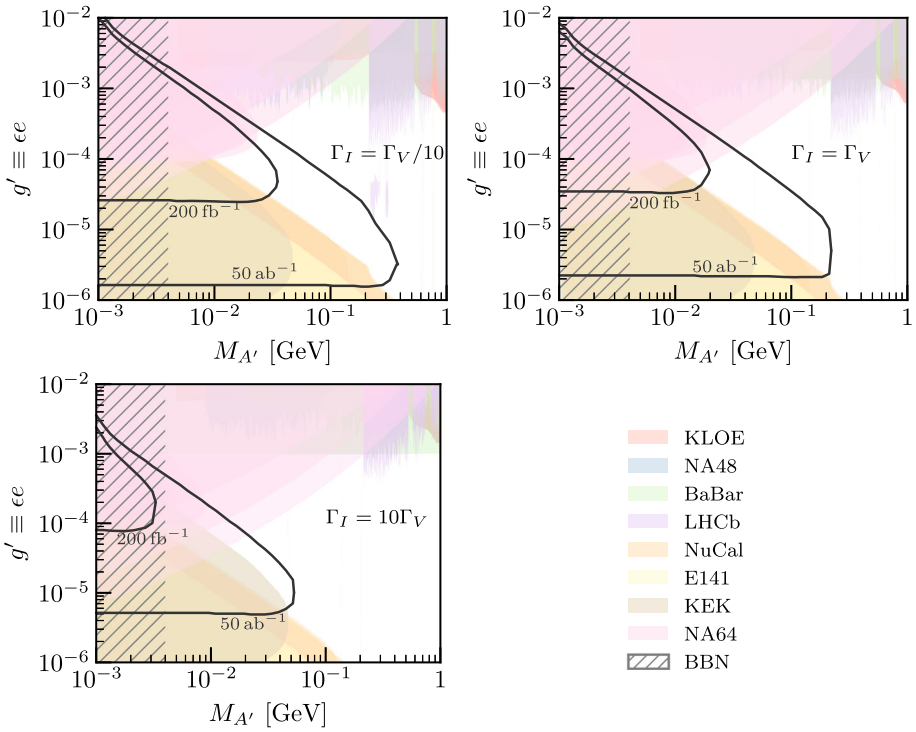

Fig. 3 We plot the 90% CL exclusion contours for different model benchmark points, viz., $\Gamma_I = \Gamma_V/10$, $\Gamma_I = \Gamma_V$, and $\Gamma_I = 10\Gamma_V$. For comparison, we have plotted the exclusion for an integrated luminosity of 200 fb^{-1} and 50 ab^{-1}. As expected, the contours weaken with reduction in branching to the visible sector and with falling luminosity. Alongside the exclusions obtained by us, we plot the exclusions already given by past experiments. In the bottom-right panel, we have given a key of the different exclusions (details in Sect. 5)

of the DP. We will give short descriptions of these limits below. The important point to pick up from the other limits is that the projections we obtain for Belle II both supplement and complement the existing limits. We will now briefly discuss the exiting bounds for completeness and reference.

5 Existing bounds and future prospects

In Fig. 3, we have plotted the contours obtained from our analysis. We have placed the contours on top of existing bounds. In this subsection, we discuss in brief the sources of these bounds. The existing bounds can be categorised as bounds from prompt searches which mostly come from detectors around interaction points, and as bounds from displaced searches, which almost exclusively come from beam dump experiments. Not surprisingly, the exclusions we obtain are mostly overlap the beam dump bounds.

5.1 Prompt

Prompt bounds come both from lepton colliders and hadron colliders. The most stringent bounds from lepton colliders are those from the BaBar experiment [34, 37, 38]. These bounds arise from the processes $e^+e^- \to A'\gamma$ and $e^+e^- \to \mu^+\mu^- A'$ and together are sensitive for $20\,\text{MeV} < M_{A'} < 10\,\text{GeV}$ and constrain till about $g' > 10^{-3}$. In Fig. 3, the green shaded region represents the bounds from BaBar. The KLOE experiment also looked for DPs in the same channel and found a bound, but for smaller windows than BaBar [35, 40]. In Fig. 3, the KLOE bounds are given in red.

For the mass range we are probing, $\pi^0/\eta \to A'\gamma$ and mixings with the ρ, ω, ϕ mesons are the primary modes of production of the DP in hadron colliders. Among the hadron colliders, the LHCb collaboration has obtained the strongest bounds on the DP parameter space [39, 42]. In Fig. 3, the violet shade gives the bound from the LHCb collaboration. The CMS collaboration has also presented bounds on the DP parameter space; however, the experiment loses sensitivity for DP masses below $\sim$ 10 GeV [60]. Recently, in Ref. [61], it has been pointed

out how machine learning techniques can be implemented to increase signal efficiency (in the context of the HL-LHC). There are bounds on the DP parameter space given by the ATLAS collaboration as well [62]. However, the exclusions are given in the context of UV models. We have to reparametrise the analysis to place the bound on top of our result. The NA48/2 [36] and the NA62 [41] experiments have looked for dark photons in the decay products of pions in prompt searches. In Fig. 3, we have shown the NA48/2 bounds in blue.

5.2 Displaced

To begin with, we have the NA64 experiment using the SPS beam at CERN. In this experiment, a 100 GeV electron beam is focussed on an active material that acts as a beam dump. The electrons (beam) lose their energy by emitting bremsstrahlung photons *and*, if present, dark photons. The DPs being weakly interacting and long lived can escape the dump. These DPs then decay to a pair of electrons and the energies of the decay products are measured in an ECAL.

A candidate $A' \to e^+e^-$ event is one where there are simultaneous showers in the dump and the ECAL, the two adding up to the beam energy. A mismatch signals channeling of energy into invisibles, leading to the bound. The bounds shaded in pink in Fig. 3 are those obtained from the NA64 experiment. As the search strategy is based on kinematic imbalance, the NA64 bound is highly sensitive to decays into the dark sector. Hence, the exclusion becomes stronger with increasing branching to the dark sector, as can be seen from Fig. 3.

Other searches at E137 [43], E141 [44], KEK [45], NuCal [46–48], Orsay [49], and APEX [50] also work on more or less the same setup and principles, while for CHARM [51] and NOMAD [52], the incident particles are protons in place of a hadrons. In Fig. 3, we have shown the exclusion contours for NuCAL (orange), E141 (brown), and KEK (yellow). We have suppressed the other exclusions as they end up constraining the same region as these three.

There is a constraint from displaced searches given by the LHCb collaboration as well [39, 42]. As of now, this region is quite small and vanishes in all cases with substantial coupling to the dark sector. In Fig. 3, this constraint is visible as an 'island' in the $\Gamma_I = \Gamma_V/10$ case only (violet).

Before ending this section, we would like to mention that alongside Ref. [55], Ref. [63] also came out, where the Belle II projections were somewhat different from those in Ref. [55]. We could not plot their contours side by side as they obtained the constraints for dark matter coupling going to zero. Qualitatively, their results indicate that Belle II is sensitive to DP masses much greater than what we get. On the other hand, their results indicate weaker sensitivity to the coupling strength than what we get.

5.3 Prospects and other analyses

It is clear that the reason that we can probe such a large region of parameter space in Belle II is because of the substantial volume of the CDC around the IP. Now, another experiment that has similar tracking abilities around the IP is GlueX at Jlab [54]. In this experiment, Bremsstrahlung photons of energy 3–12 GeV (6–22 GeV in the near future [64]) are incident on hydrogen nuclei (or heavy ions). Integrated luminosity is expected to reach above ~ 1 fb^{-1}. Like Belle II, GlueX has a central drift chamber around the interaction point, the details of which are given in Table 2.

The CoM energy in Table 2 assumes that the target is proton, it will increase for heavy ions. Our initial analysis for GlueX shows that it is almost as sensitive to the displaced vertex signatures of the DP as is Belle II. The slight disadvantage it has is due to its lower CoM energy compared to Belle II. We will soon make our findings public. Note, as GlueX employs fixed target collisions, the final state particles have significant forward activity. To register the tracks due to these particles, the experiment has installed a forward tracker with substantial fiducial volume. We are yet to analyse the sensitivity of this tracker to DP displaced vertices and, hence, have not included details of this part in Table 2.

Not only GlueX, the FASER detector at LHC has recently started publishing their DP results and although, as of now, these bounds are not much stronger than existing ones, with more data taking it is bound to cover vast regions of the uncharted parameter space [65]. Other LHC annex experiments like MATHUSLA [66] and CODEX-b [67] have also been commissioned/proposed to look for long-lived particles and will no doubt expand

Table 2 Some details of the GlueX experiment

$\sqrt{s}$	Integrated Luminosity	Active CDC Dimensions		
		Radial (cm)	Axial (cm)	Angular
3.6 GeV – 7 GeV	Few fb^{-1}	$10 < r < 50$	$-50 < z < 100$	$20^\circ < \theta < 132^\circ$

on the parameter space probed as of now. Dark Photons have also been considered in the context of proposed experiments, like the FCC-hh [68], at the EIC [69], and the ILC (and FCC-ee, CEPC) [2, 70].

6 Conclusions

The region of unexplored parameter space for a dark photon like particle lends itself well to displaced vertex searches. With this identification, we have discussed the sensitivity of the Belle II CDC towards such vertices. To do so, we have assumed models where the DP is a portal between the visible and the dark sector and have studied different scenarios parametrised by the relative widths of the dark photon to the visible and the invisible sectors. We find the sensitivity of Belle II to complement the existing bounds for large regions of the parameter space. Our positive findings behove the Belle II collaboration to analyse their data for displaced vertices of dark photons decaying to charged leptons. We concluded that with Belle II alongside a plethora of other experiments equipped to reconstruct displaced vertices, we are certain to probe extended regions of the unexplored dark photon parameter space in the current decade.

Acknowledgements The author acknowledges Sabyasachi Chakraborty and Sokratis Trifinopoulos for their contributions to the development of the analysis techniques and Igal Jaegle for pointing out the suitability of the GlueX experiment.

Data availability statement Data sets generated during the current study are available from the corresponding author upon reasonable request.

References

1. R.L. Workman, et al. Review of particle physics. PTEP 2022, 083–01 (2022). https://doi.org/10.1093/ptep/ptac097
2. K. Asai, S. Iwamoto, Y. Sakaki, D. Ueda, New physics searches at the ILC positron and electron beam dumps. JHEP **09**, 183 (2021). https://doi.org/10.1007/JHEP09(2021)183. arXiv:2105.13768 [hep-ph]
3. T. Bose, et al., Report of the topical group on physics beyond the standard model at energy frontier for snowmass 2021 (2022). arXiv:2209.13128 [hep-ph]
4. S. Sekmen, Highlights on supersymmetry and exotic searches at the LHC (2022). arXiv:2204.03053 [hep-ex]
5. P.J. Fox, et al. TF08 snowmass report: bsm model building (2022). arXiv:2210.03075 [hep-ph]
6. H. Georgi, D.B. Kaplan, L. Randall, Manifesting the invisible axion at low-energies. Phys. Lett. B **169**, 73–78 (1986). https://doi.org/10.1016/0370-2693(86)90688-X
7. L.M. Krauss, D.J. Nash, A viable weak interaction axion? Phys. Lett. B **202**, 560–567 (1988). https://doi.org/10.1016/0370-2693(88)91864-3
8. H. Fukuda, K. Harigaya, M. Ibe, T.T. Yanagida, Model of visible QCD axion. Phys. Rev. D **92**(1), 015021 (2015). https://doi.org/10.1103/PhysRevD.92.015021. arXiv:1504.06084 [hep-ph]
9. D.S.M. Alves, N. Weiner, A viable QCD axion in the MeV mass range. JHEP **07**, 092 (2018). https://doi.org/10.1007/JHEP07(2018)092. arXiv:1710.03764 [hep-ph]
10. M. Bauer, M. Neubert, S. Renner, M. Schnubel, A. Thamm, Consistent treatment of axions in the weak chiral lagrangian. Phys. Rev. Lett. **127**(8), 081803 (2021). https://doi.org/10.1103/PhysRevLett.127.081803. arXiv:2102.13112 [hep-ph]
11. T. Bandyopadhyay, S. Ghosh, T.S. Roy, ALP-Pions generalized. Phys. Rev. D **105**(11), 115039 (2022). https://doi.org/10.1103/PhysRevD.105.115039. arXiv:2112.13147 [hep-ph]
12. L.B. Okun, Limits of electrodynamics: paraphotons? Sov. Phys. JETP **56**, 502 (1982)
13. P. Galison, A. Manohar, Two z's or not two z's? Phys. Lett. B **136**, 279–283 (1984). https://doi.org/10.1016/0370-2693(84)91161-4
14. B. Holdom, Two U(1)'s and epsilon charge shifts. Phys. Lett. B **166**, 196–198 (1986). https://doi.org/10.1016/0370-2693(86)91377-8
15. P. Fayet, On the search for a new spin 1 boson. Nucl. Phys. B **187**, 184–204 (1981). https://doi.org/10.1016/0550-3213(81)90122-X
16. R. Foot, New physics from electric charge quantization? Mod. Phys. Lett. A **6**, 527–530 (1991). https://doi.org/10.1142/S0217732391000543
17. X.G. He, G.C. Joshi, H. Lew, R.R. Volkas, New Z-prime phenomenology. Phys. Rev. D **43**, 22–24 (1991). https://doi.org/10.1103/PhysRevD.43.R22
18. X.-G. He, G.C. Joshi, H. Lew, R.R. Volkas, Simplest Z-prime model. Phys. Rev. D **44**, 2118–2132 (1991). https://doi.org/10.1103/PhysRevD.44.2118
19. H.-C. Cheng, L. Li, E. Salvioni, A theory of dark pions. JHEP **01**, 122 (2022). https://doi.org/10.1007/JHEP01(2022)122. arXiv:2110.10691 [hep-ph]

20. J.L. Feng, B. Fornal, I. Galon, S. Gardner, J. Smolinsky, T.M.P. Tait, P. Tanedo, Protophobic fifth-force interpretation of the observed anomaly in ^{8}Be nuclear transitions. Phys. Rev. Lett. **117**(7), 071803 (2016). https://doi.org/10.1103/PhysRevLett.117.071803. arXiv:1604.07411 [hep-ph]
21. J.L. Feng, B. Fornal, I. Galon, S. Gardner, J. Smolinsky, T.M.P. Tait, P. Tanedo, Particle physics models for the 17 MeV anomaly in beryllium nuclear decays. Phys. Rev. D **95**(3), 035017 (2017). https://doi.org/10.1103/PhysRevD.95.035017. arXiv:1608.03591 [hep-ph]
22. C. Boehm, P. Fayet, Scalar dark matter candidates. Nucl. Phys. B **683**, 219–263 (2004). https://doi.org/10.1016/j.nuclphysb.2004.01.015. arXiv:hep-ph/0305261
23. P. Fayet, Light spin 1/2 or spin 0 dark matter particles. Phys. Rev. D **70**, 023514 (2004). https://doi.org/10.1103/PhysRevD.70.023514. arXiv:hep-ph/0403226
24. Y. Nomura, J. Thaler, Dark Matter through the Axion Portal. Phys. Rev. D **79**, 075008 (2009) https://doi.org/10.1103/PhysRevD.79.075008. arXiv:0810.5397 [hep-ph]
25. Y. Hochberg, E. Kuflik, R. Mcgehee, H. Murayama, K. Schutz, Strongly interacting massive particles through the axion portal. Phys. Rev. D **98**(11), 115031 (2018). https://doi.org/10.1103/PhysRevD.98.115031. arXiv:1806.10139 [hep-ph]
26. C.A. Manzari, J. Martin Camalich, J. Spinner, R. Ziegler, Supernova limits on muonic dark forces. Phys. Rev. D **108**(10), 103020 (2023). https://doi.org/10.1103/PhysRevD.108.103020. arXiv:2307.03143 [hep-ph]
27. D.P. Aguillard et al., Measurement of the positive muon anomalous magnetic moment to 0.20 ppm (2023). arXiv:2308.06230 [hep-ex]
28. A.J. Krasznahorkay et al., New results on the ^{8}Be anomaly. J. Phys. Conf. Ser. **1056**(1), 012028 (2018). https://doi.org/10.1088/1742-6596/1056/1/012028
29. A.J. Krasznahorkay, M. Csatlós, L. Csige, J. Gulyás, A. Krasznahorkay, B.M. Nyakó, I. Rajta, J. Timár, I. Vajda, N.J. Sas, New anomaly observed in He4 supports the existence of the hypothetical X17 particle. Phys. Rev. C **104**(4), 044003 (2021). https://doi.org/10.1103/PhysRevC.104.044003. arXiv:2104.10075 [nucl-ex]
30. T. Aaltonen et al., High-precision measurement of the W boson mass with the CDF II detector. Science **376**(6589), 170–176 (2022). https://doi.org/10.1126/science.abk1781
31. T. Bandyopadhyay, A. Budhraja, S. Mukherjee, T.S. Roy, A twisted tale of the transverse-mass tail. JHEP **08**, 135 (2023). https://doi.org/10.1007/JHEP08(2023)135. arXiv:2212.02534 [hep-ph]
32. A. Crivellin, B. Mellado, Anomalies in particle physics (2023). arXiv:2309.03870 [hep-ph]
33. W. Altmannshofer, et al. The belle II physics book. PTEP **2019**(12), 123–01 (2019). https://doi.org/10.1093/ptep/ptz106. arXiv:1808.10567 [hep-ex]. [Erratum: PTEP 2020, 029201 (2020)]
34. J.P. Lees et al., Search for a dark photon in e^+e^- collisions at BaBar. Phys. Rev. Lett. **113**(20), 201801 (2014). https://doi.org/10.1103/PhysRevLett.113.201801. arXiv:1406.2980 [hep-ex]
35. A. Anastasi, et al. Limit on the production of a low-mass vector boson in $e^+e^- \to U\gamma$, $U \to e^+e^-$ with the KLOE experiment. Phys. Lett. B **750**, 633–637 (2015). https://doi.org/10.1016/j.physletb.2015.10.003. arXiv:1509.00740 [hep-ex]
36. J.R. Batley, et al. Search for the dark photon in π^0 decays. Phys. Lett. B **746**, 178–185 (2015). https://doi.org/10.1016/j.physletb.2015.04.068. arXiv:1504.00607 [hep-ex]
37. J.P. Lees et al., Search for a muonic dark force at BABAR. Phys. Rev. D **94**(1), 011102 (2016). https://doi.org/10.1103/PhysRevD.94.011102. arXiv:1606.03501 [hep-ex]
38. J.P. Lees et al., Search for invisible decays of a dark photon produced in e^+e^- collisions at BaBar. Phys. Rev. Lett. **119**(13), 131804 (2017). https://doi.org/10.1103/PhysRevLett.119.131804. arXiv:1702.03327 [hep-ex]
39. R. Aaij et al., Search for dark photons produced in 13 TeV pp collisions. Phys. Rev. Lett. **120**(6), 061801 (2018). https://doi.org/10.1103/PhysRevLett.120.061801. arXiv:1710.02867 [hep-ex]
40. A. Anastasi, *et al.* Combined limit on the production of a light gauge boson decaying into $\mu^+\mu^-$ and $\pi^+\pi^-$. Phys. Lett. B **784**, 336–341 (2018). https://doi.org/10.1016/j.physletb.2018.08.012. arXiv:1807.02691 [hep-ex]
41. E. Cortina Gil, et al., Search for production of an invisible dark photon in π^0 decays. JHEP **05**, 182 (2019). https://doi.org/10.1007/JHEP05(2019)182. arXiv:1903.08767 [hep-ex]
42. R. Aaij et al., Search for $A' \to \mu^+\mu^-$ Decays. Phys. Rev. Lett. **124**(4), 041801 (2020). https://doi.org/10.1103/PhysRevLett.124.041801. arXiv:1910.06926 [hep-ex]
43. J.D. Bjorken, S. Ecklund, W.R. Nelson, A. Abashian, C. Church, B. Lu, L.W. Mo, T.A. Nunamaker, P. Rassmann, Search for neutral metastable penetrating particles produced in the SLAC beam dump. Phys. Rev. D **38**, 3375 (1988). https://doi.org/10.1103/PhysRevD.38.3375
44. E.M. Riordan et al., A search for short lived axions in an electron beam dump experiment. Phys. Rev. Lett. **59**, 755 (1987). https://doi.org/10.1103/PhysRevLett.59.755
45. A. Konaka et al., Search for neutral particles in electron beam dump experiment. Phys. Rev. Lett. **57**, 659 (1986). https://doi.org/10.1103/PhysRevLett.57.659
46. J. Blumlein et al., Limits on neutral light scalar and pseudoscalar particles in a proton beam dump experiment. Z. Phys. C **51**, 341–350 (1991). https://doi.org/10.1007/BF01548556
47. J. Blumlein et al., Limits on the mass of light (pseudo)scalar particles from Bethe-Heitler e+ e- and mu+ mu- pair production in a proton - iron beam dump experiment. Int. J. Mod. Phys. A **7**, 3835–3850 (1992). https://doi.org/10.1142/S0217751X9200171X

48. Y.-D. Tsai, P. deNiverville, M.X. Liu, Dark photon and muon $g-2$ inspired inelastic dark matter models at the high-energy intensity frontier. Phys. Rev. Lett. **126**(18), 181801 (2021). https://doi.org/10.1103/PhysRevLett.126.181801. arXiv:1908.07525 [hep-ph]
49. M. Davier, H. Nguyen Ngoc, An Unambiguous Search for a Light Higgs Boson. Phys. Lett. B **229**, 150–155 (1989). https://doi.org/10.1016/0370-2693(89)90174-3
50. S. Abrahamyan, et al. Search for a new gauge boson in electron-nucleus fixed-target scattering by the APEX experiment. Phys. Rev. Lett. **107**, 191804 (2011). https://doi.org/10.1103/PhysRevLett.107.191804. arXiv:1108.2750 [hep-ex]
51. F. Bergsma et al., Search for Axion like particle production in 400-GeV proton-copper interactions. Phys. Lett. B **157**, 458–462 (1985). https://doi.org/10.1016/0370-2693(85)90400-9
52. S.N. Gninenko, Stringent limits on the $\pi^0 \to \gamma X$, $X \to e+e-$ decay from neutrino experiments and constraints on new light gauge bosons. Phys. Rev. D **85**, 055027 (2012). https://doi.org/10.1103/PhysRevD.85.055027. arXiv:1112.5438 [hep-ph]
53. M. Ablikim et al., Future Physics Programme of BESIII. Chin. Phys. C **44**(4), 040001 (2020). https://doi.org/10.1088/1674-1137/44/4/040001. arXiv:1912.05983 [hep-ex]
54. S. Adhikari, *et al.* The GLUEX beamline and detector. Nucl. Instrum. Meth. A **987**, 164807 (2021). https://doi.org/10.1016/j.nima.2020.164807. arXiv:2005.14272 [physics.ins-det]
55. T. Bandyopadhyay, S. Chakraborty, S. Trifinopoulos, Displaced searches for light vector bosons at Belle II. JHEP **05**, 141 (2022). https://doi.org/10.1007/JHEP05(2022)141. arXiv:2203.03280 [hep-ph]
56. P. Ilten, Y. Soreq, M. Williams, W. Xue, Serendipity in dark photon searches. JHEP **06**, 004 (2018). https://doi.org/10.1007/JHEP06(2018)004. arXiv:1801.04847 [hep-ph]
57. T. Fujiwara, T. Kugo, H. Terao, S. Uehara, K. Yamawaki, Nonabelian anomaly and vector mesons as dynamical gauge bosons of hidden local symmetries. Prog. Theor. Phys. **73**, 926 (1985). https://doi.org/10.1143/PTP.73.926
58. E. Bertholet, S. Chakraborty, V. Loladze, T. Okui, A. Soffer, K. Tobioka, Heavy QCD axion at belle II: displaced and prompt signals (2021). arXiv:2108.10331 [hep-ph]
59. N. Sabti, J. Alvey, M. Escudero, M. Fairbairn, D. Blas, Refined bounds on MeV-scale thermal dark sectors from BBN and the CMB. JCAP **01**, 004 (2020). https://doi.org/10.1088/1475-7516/2020/01/004. arXiv:1910.01649 [hep-ph]
60. Search for long-lived particles decaying to a pair of muons in pp collisions at $\sqrt{s} = 13.6$ TeV with 2022 data. Technical report, CERN, Geneva (2023). https://cds.cern.ch/record/2868338
61. Bhattacherjee, B., Konar, P., Ngairangbam, V.S., Solanki, P.: LLPNet: Graph autoencoder for triggering light long-lived particles at HL-LHC (2023). arXiv:2308.13611 [hep-ph]
62. G. Aad, et al. Search for light long-lived neutral particles that decay to collimated pairs of leptons or light hadrons in pp collisions at $\sqrt{s} = 13$ TeV with the ATLAS detector. JHEP **06**, 153 (2023). https://doi.org/10.1007/JHEP06(2023)153. arXiv:2206.12181 [hep-ex]
63. T. Ferber, C. Garcia-Cely, K. Schmidt-Hoberg, BelleII sensitivity to long–lived dark photons. Phys. Lett. B **833**, 137373 (2022). https://doi.org/10.1016/j.physletb.2022.137373. arXiv:2202.03452 [hep-ph]
64. A. Accardi, et al. Strong interaction physics at the luminosity frontier with 22 GeV electrons at jefferson lab (2023). arXiv:2306.09360 [nucl-ex]
65. H. Abreu, et al. Search for dark photons with the FASER detector at the LHC (2023). arXiv:2308.05587 [hep-ex]
66. D. Curtin et al., Long-lived particles at the energy frontier: the MATHUSLA physics case. Rept. Prog. Phys. **82**(11), 116201 (2019). https://doi.org/10.1088/1361-6633/ab28d6. arXiv:1806.07396 [hep-ph]
67. V.V. Gligorov, S. Knapen, M. Papucci, D.J. Robinson, Searching for long-lived particles: a compact detector for exotics at LHCb. Phys. Rev. D **97**(1), 015023 (2018). https://doi.org/10.1103/PhysRevD.97.015023. arXiv:1708.09395 [hep-ph]
68. B. Bhattacherjee, H.K. Dreiner, N. Ghosh, S. Matsumoto, R. Sengupta, P. Solanki, Light long-lived particles at the FCC-hh with the proposal for a dedicated forward detector FOREHUNT and a transverse detector DELIGHT (2023). arXiv:2306.11803 [hep-ph]
69. H. Davoudiasl, R. Marcarelli, E.T. Neil, Displaced signals of hidden vectors at the electron-ion collider (2023). arXiv:2307.00102 [hep-ph]
70. R. Schäfer, F. Tillinger, S. Westhoff, Near or far detectors? A case study for long-lived particle searches at electron-positron colliders. Phys. Rev. D **107**(7), 076022 (2023). https://doi.org/10.1103/PhysRevD.107.076022. arXiv:2202.11714 [hep-ph]